

Some features of the reaction $pp \rightarrow \Delta^{++}(1236)n$ at 6 GeV/c*

J. D. Mountz[†] and Gerald A. Smith

Department of Physics, Michigan State University, East Lansing, Michigan 48824

A. J. Lennox, J. A. Poirier, J. P. Prukop,[‡] C. A. Rey, and O. R. Sander[§]

Department of Physics, University of Notre Dame, Notre Dame, Indiana 46556

P. Kirk,^{||} R. D. Klem, and Irwin Spirn

Argonne National Laboratory, Argonne, Illinois 60439

(Received 28 April 1975)

Approximately 12000 examples of the reaction $pp \rightarrow \Delta^{++}(1236)n$ have been identified at 6 GeV/c in a spark-chamber experiment performed at the Argonne National Laboratory Zero Gradient Synchrotron. The experimental invariant-mass and momentum-transfer-squared distributions are in agreement with predictions of the Chew-Low one-pion-exchange model, suitably modified to account for form factors or absorption. The data have been extrapolated from the physical region to the pion pole. It is found that the Dürr-Pilkuhn and Benecke-Dürr models, in conjunction with quadratic extrapolations in t , reproduce the known on-mass-shell dependence of the cross section for the elastic π^+p scattering.

I. INTRODUCTION

This paper reports on an analysis of 12 271 events of the type



The dominant one-pion-exchange (OPE) diagram for this reaction is shown in Fig. 1. The distributions for the $p\pi^+$ invariant mass, $M_{p\pi}$, and the momentum transfer squared from the target proton to the recoil neutron, t , are compared with predictions of the Dürr-Pilkuhn¹ and Benecke-Dürr² models. Both of these models are form-factor models which effectively absorb the low partial waves in the context of the OPE model. Good agreement is seen between the data and the distributions predicted by these models.

Chew and Low have proposed a scheme for measuring physical cross sections using virtual-particle states as targets.³ In a scattering reaction, the square of the mass of the virtual exchange particle (target) is identical to the square of the momentum transfer from the real target particle to the recoil particle. The physical cross section

for the virtual target is obtained by extrapolating t , measured in the scattering reaction, into the unphysical t region. This extrapolated cross section can be evaluated at $t = +\mu^2$, where μ is the mass of the exchange particle, to obtain the on-shell cross section.^{4,5} In the case of reaction (1), the $M_{p\pi}$ and t distributions derive their shape from a combined contribution of the $pn\pi^+$ vertex, the pion propagator, the $p\pi\Delta^{++}$ vertex, and dynamical form factors.⁶ A meaningful extrapolation of the data cannot be done unless the t distribution is linearized by normalizing the data with different models. The Chew-Low model³ considers only the kinematics of OPE, whereas the Dürr-Pilkuhn¹ and Benecke-Dürr² models introduce additional form factors to help linearize the extrapolation curves. Finally, the extrapolated results for π^+p scattering obtained with the aid of these different models are compared with known on-mass-shell cross sections^{7,8} as a measure of the success of the over-all technique.

II. ONE-PION EXCHANGE AND POLE EXTRAPOLATION

In terms of notation used subsequently in this paper, we define the four-vector for a particle of energy E and three-momentum \vec{P} as $P = (E, i\vec{P})$. All vectors are expressed in the over-all center-of-mass system unless otherwise noted. The beam, target, neutron, pion, and proton four-momenta are written as $P_B, P_T, P_n, P_\pi,$ and P_p , respectively. The rest masses for the proton, neutron, and pion are given by $M_p, M_n,$ and μ , respectively. The quantity P_L is the laboratory momentum of the beam particle. In terms of the center-of-mass four-vectors, one can write the

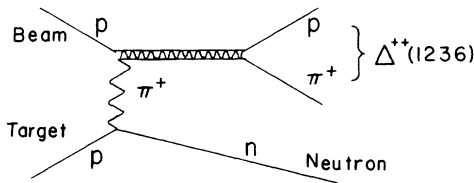


FIG. 1. One-pion-exchange (OPE) diagram for reaction (1).

square of the mass of the p - π^+ system, denoted by $M_{p\pi}^2$, as

$$M_{p\pi}^2 = (P_p + P_\pi)^2. \quad (2)$$

The momentum transfer squared from the target proton to the neutron, denoted by t , is

$$t = (P_n - P_T)^2. \quad (3)$$

The decay angles of the Δ^{++} are defined in the Gottfried-Jackson frame.⁹ The two decay angles are taken to be the scattering angle of the beam proton in the Δ^{++} center-of-mass system, or Jackson angle, denoted by θ_J , and the azimuthal angle, or Treiman-Yang angle, denoted by ϕ_{TY} . These angles are defined as

$$\cos\theta_J = \frac{\vec{P}_B \cdot \vec{P}_p}{|\vec{P}_B \cdot \vec{P}_p|} \quad (4)$$

and

$$\cos\phi_{TY} = \frac{(\vec{P}_T \times \vec{P}_n) \cdot (\vec{P}_B \times \vec{P}_p)}{|\vec{P}_T \times \vec{P}_n| |\vec{P}_B \times \vec{P}_p|}. \quad (5)$$

The on-mass-shell pion momentum in the Δ^{++} center-of-mass system is denoted by Q , where

$$Q = R(M_p, \mu, M_{p\pi}) \quad (6)$$

and

$$R(M_1, M_2, M_3) = \{[(M_3 - M_2)^2 - M_1^2][(M_3 + M_2)^2 - M_1^2]\}^{1/2} / (2M_3). \quad (7)$$

The off-mass-shell pion momentum in the Δ^{++} center-of-mass system, Q_t , is given by

$$Q_t = R(M_p, t, M_{p\pi}). \quad (8)$$

The on-mass-shell and off-mass-shell pion momentum in the neutron center-of-mass system are given by

$$q = R(M_p, \mu, M_n) \quad (9)$$

and

$$q_t = R(M_p, t, M_n), \quad (10)$$

respectively.

Turning now to the dynamics of reaction (1), the cross section for this process, in the Born approximation, is given by¹⁰⁻¹²

$$\begin{aligned} \left(\frac{d^2\sigma}{dM_{p\pi} dt} \right)_B &= \frac{1}{2\pi M_p^2 P_L^2} \left(\frac{G_{pn\pi}^2}{4\pi} \right) \frac{t}{(t - \mu^2)^2} \\ &\times Q M_{p\pi}^2 \sigma(M_{p\pi}) \\ &\times \left[\frac{Q_t^2}{Q^2} \frac{(M_p + M_{p\pi})^2 - t}{(M_p + M_{p\pi})^2 - \mu^2} \right]. \quad (11) \end{aligned}$$

The factor in the square brackets results from the Δ^{++} vertex calculation. The pseudoscalar pion

exchange factor from the $pn\pi^+$ vertex contributes the t to the cross section and $(t - \mu^2)^{-2}$ is the square of the pion propagator. The quantity $G_{pn\pi}^2/(4\pi)$ is the coupling constant for the charged pion to the nucleon, and is taken to be 29.2. The quantity $\sigma(M_{p\pi})$ is the on-mass-shell elastic π^+p scattering cross section.⁸ At the pion pole, the quantity in the square brackets reduces to one and the remainder of Eq. (11) is called the pole equation or Chew-Low formula.³

Dürr and Pilkuhn¹ utilize a technique well known to nuclear physics¹³ to arrive at a vertex correction which introduces form factors for $r < R_0$, where r is the pion-nucleon separation and R_0 is the interactive radius of the nucleon. The form factors obtained for the Δ^{++} vertex and the $pn\pi^+$ vertex are

$$F_{p\Delta\pi}^{DP}(t) = \frac{1 + R_\Delta^2 Q^2}{1 + R_\Delta^2 Q_t^2} \quad (12)$$

and

$$F_{pn\pi}^{DP}(t) = \frac{1 + R_n^2 q^2}{1 + R_n^2 q_t^2}, \quad (13)$$

where R_Δ is the radius associated with the $p\Delta\pi$ vertex, taken⁴ to be 4.0 GeV⁻¹, and R_n is the nucleon radius, taken⁴ to be 2.66 GeV⁻¹. Benecke and Dürr² derived form factors which can be used for a resonance vertex to account for finite extension of the strongly interacting matter. For scattering at a vertex with definite angular momentum l , the form factor is

$$F_l^{BD}(t) = \frac{u_l(QR)}{u_l(Q_t R)}, \quad (14)$$

where Q , Q_t , and R conform with previous definitions and

$$u_l(x) = \left(\frac{1}{2x^2} \right) Q_t \left(1 + \frac{1}{2x^2} \right). \quad (15)$$

The quantities $Q_l(x)$ are Legendre functions of the second kind. For the Δ^{++} vertex, where $l=1$, one has

$$u_1(x) = \frac{1}{2x^2} \left[\frac{2x^2 + 1}{4x^2} \ln(4x^2 + 1) - 1 \right], \quad (16)$$

and R_Δ is taken⁴ as 2.2 GeV⁻¹.

The pole extrapolation procedure can be illustrated by using the pole equation and the various off-shell effects as described above. The quantity " $t\sigma$ " can be factored out of the pole equation (11) to give⁵

$$"t\sigma" = \frac{N/S}{\int dM_{p\pi} dt} \frac{2\pi M_p^2 P_L^2 (t - \mu^2)^2}{(G_{pn\pi}^2/4\pi) Q M_{p\pi}^2}. \quad (17)$$

To evaluate " $t\sigma$ ", the experimental off-shell scattering data are divided into bins of $M_{p\pi}$ and t , with

N the number of events in a particular bin and S the cross-section normalization factor expressed in mb/event. The expression $\int dM_{p\pi} dt$ is taken over the portion of phase space experimentally accessible after kinematical restrictions are considered. The average of the factors on the right-hand side of the equation is used to represent σ at the average t and $M_{p\pi}$ of the interval. The form factors can be incorporated into the above expression to give a smoother off-shell t dependence for the data. An additional universal weakly t -dependent form factor,

$$g^2(t) = [(C - \mu^2)/(C - t)]^2, \quad (18)$$

is used in the pole extrapolation with C set⁴ at 2.3 GeV². This form factor, introduced by Wolf⁴ in an *ad hoc* fashion, provides a very weak t -dependent correction to the previously discussed form factors in the Chew-Low, Dürr-Pilkuhn, and Benecke-Dürr models.

III. EXPERIMENT AND DATA ANALYSIS

A proton beam from the Argonne National Laboratory Zero Gradient Synchrotron of momentum $6 \pm 0.5\%$ GeV/ c was focused into a six-in. long hydrogen target. Figure 2 shows an over-all plan of the apparatus. The momentum analyzing magnet (SCM-105) had a ± 44 in. horizontal and ± 13 in. vertical aperture with a central field of 8 kG and an effective magnetic field length of 40 in.

The counters used to trigger the apparatus are shown by the solid lines in Fig. 2. The beam telescope (B_1 and B_2), hodoscope counters (H_i), and anticounter (A) were constructed using one-quarter in. scintillator bonded to notched Lucite

cylindrical lightpipes. The counter A had a one-in. hole drilled in its center with photomultipliers attached to two opposite sides. The hodoscope array, H_i , was designed to have a high two-track acceptance. The dE/dx counter (D) selected multiple charged final states and rejected noninteracting beam particles. A trigger was defined as $\bar{C}B_1B_2\bar{A}(D>1)H_iH_j$, where $D>1$ required more than one particle in the dE/dx counter, H_iH_j required the firing of two or more separate hodoscope elements, and \bar{C} indicated that a proton had traversed the threshold Čerenkov counter in the beam.

The ten wire spark chambers used in this experiment, shown as dotted lines in Fig. 2, had 48 wires/in. crossing magnetostrictive wands. Each spark chamber consisted of two planes of wires pulsed at a nominal 5-kV potential. Unambiguous spatial location determination for two-track final states demanded that some chambers have nonorthogonal wire orientation. Planes 9–20 (spark chambers 5–10) were used with four scalers apiece, recording up to four sparks per plane. The total data from the twenty planes were read onto magnetic tape by the Varian 620/ i mini-computer. Typically 15 triggers per beam burst were recorded over a beam spill time of 500 msec, resulting in 1.469×10^6 analyzed triggers. The total number of beam protons incident on the target was 139.3×10^6 , leading to an event cross-section normalization of 1.113×10^{-5} mb/event.

The triggers were analyzed through the filter program CRUNCH,¹⁴ which attempted to find two tracks and identify the X - Y - Z positions at the spark chambers for the tracks in the event. The over-all transmission of triggers to two-prong

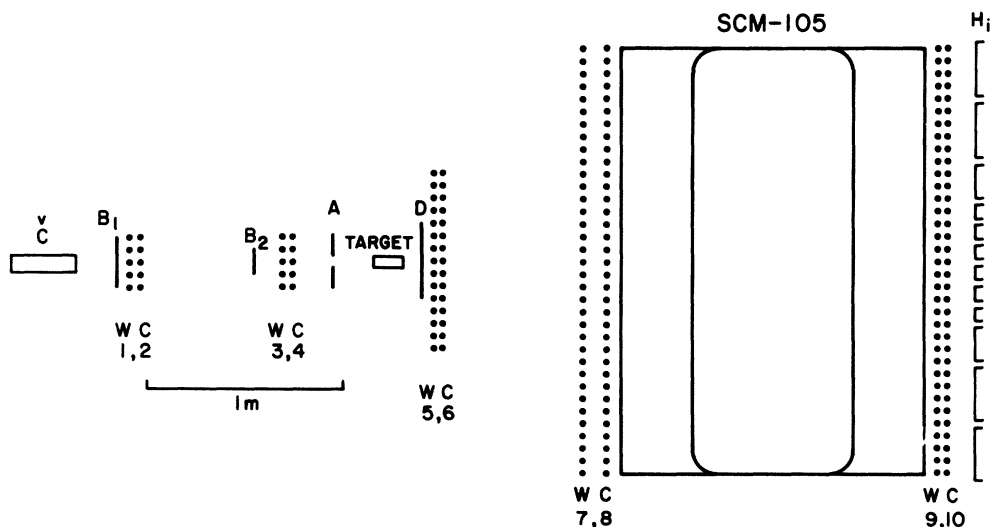


FIG. 2. Plan view of the magnetostrictive spark-chamber apparatus used in this experiment.

events was found to be 17%. At this point, no selections on the sign of the charge or kinematic restrictions were imposed. The program CIRCE is a general multiprong computer program designed for a nonuniform magnetic field.^{15,16} For this experiment it was altered to take the X - Y - Z values and errors in these quantities for the input beam track and two outgoing tracks and return a curvature, dip, and azimuth angle for each track, as well as the vertex and a 12×12 correlated error matrix. The 32% reduction of triggers from CRUNCH to CIRCE was due to one or two negative tracks in the final state.

The program TEUTA¹⁷ attempted to fit the output CIRCE events to the following hypotheses:

$$pp \rightarrow pn\pi^+, \quad (19)$$

$$\rightarrow \pi^+ np, \quad (20)$$

$$\rightarrow pp\pi^0, \quad (21)$$

and

$$\rightarrow pp. \quad (22)$$

A 3% confidence level cut resulted in 31 908 $pn\pi^+$ events and 6830 $pp\pi^0$ events. The $\Delta^{++}n$ sample was obtained by requiring $t < 0.3 \text{ GeV}^2$ and $1.14 < M_{p\pi} < 1.42 \text{ GeV}$. These cuts resulted in 12 271 events. The possible ambiguity between reactions (19) and (20) was studied in terms of Monte Carlo events. The study showed that when the proton and pion were interchanged, the two-particle invariant mass was no longer in the Δ^{++} region. In fact, under these conditions the mass becomes quite large, approaching the kinematic limit. It was also observed that the loss of events due to this interchange resulted in a nearly uniform depletion of events across the Δ^{++} mass region and the corresponding t distribution. It was concluded that the loss of events from reaction (1) was correctable by a simple multiplicative factor which was independent of the shapes of the $M_{p\pi}$ and t distributions.

It was observed that the apparatus had a limited acceptance for certain wide-angle and low-momentum tracks. However, the large X - Y plane acceptance ensured that wide-angle tracks were recorded in this orientation, and the losses from the vertical X - Z orientation were calculable by a rotation about the beam axis. An acceptance weight equal to the inverse of the probability of detecting the event was assigned to each event. It was also found that the apparatus used in this experiment had zero acceptance for some small percentage of tracks of reaction (1). On the basis of Monte Carlo data, an efficiency curve was derived as a function of the $M_{p\pi}$, t , θ_J , and ϕ_{TY} variables. The cross-section correction due to

zero acceptance was 13% for $1.14 < M_{p\pi} < 1.42 \text{ GeV}$, the mass range used in this analysis.

The Monte Carlo events were also used to obtain a 3% pion decay correction, a 3% Coulomb scattering correction,¹⁸⁻²⁰ and a 7% strong scattering correction for secondary tracks. A spark-chamber efficiency of 88.5% was calculated assuming three or four spark-chamber firings per track for the beam and premagnet sections and one or two spark-chamber firings per track for the post-magnet section. The dE/dx efficiency calculation took into account the Landau energy fluctuation of energy loss by a particle through the scintillator,²¹ as well as scintillator efficiency and photon production spectrum, lightpipe efficiency, and phototube efficiency.^{22,23} Figures 3(a)-3(d) show the distributions of the four independent variables used in this analysis before (shaded) and after (all) experimental corrections.

In addition to the aforementioned corrections, a factor of 2 was used in the cross-section calculation because no center-of-mass backward hemisphere $\Delta^{++}n$ events were seen by the apparatus. The cross section for reaction (1) was measured to be

$$\sigma(\Delta^{++}n) = 2.70 \pm 0.15 \text{ mb}. \quad (23)$$

An additional correction factor of 1.476 was applied to compensate for the mass cut $1.14 < M_{p\pi} \leq 1.42 \text{ GeV}$, based on Breit-Wigner fits discussed in the next section. No correction was made for the $-t < 0.3 \text{ GeV}^2$ cut. This cross section is plotted with other experimental points between 1 and 10 GeV/c in Fig. 4, and appears to be in excellent agreement with the over-all trend of the data.²⁴

IV. DIFFERENTIAL CROSS SECTIONS AND POLE EXTRAPOLATION

The $M_{p\pi}$ and t distributions for reaction (1) are shown in Fig. 5(a) and 5(b) and tabulated in Tables I and II. The solid curves are predictions of the Dürr-Pilkuhn form factor model. The prominent $\Delta^{++}(1236)$ resonance evident in the $M_{p\pi}$ distribution was fitted to a Breit-Wigner form,

$$\sigma(M_{p\pi}^2) \propto \frac{M_0 \Gamma}{(M_{p\pi}^2 - M_0^2)^2 + (M_0 \Gamma)^2},$$

where

$$\Gamma = \Gamma_0 \left(\frac{QR}{Q_0 R} \right)^3 \left\{ \frac{1 + (Q_0 R)^2}{1 + (QR)^2} \right\}. \quad (24)$$

The results, corrected for effects of resolution, give peak and FWHM values of $1.226 (\pm 0.004) \text{ GeV}$ and $0.126 (\pm 0.006) \text{ GeV}$, respectively. In general, the data and Dürr-Pilkuhn model predictions are in good agreement, although an

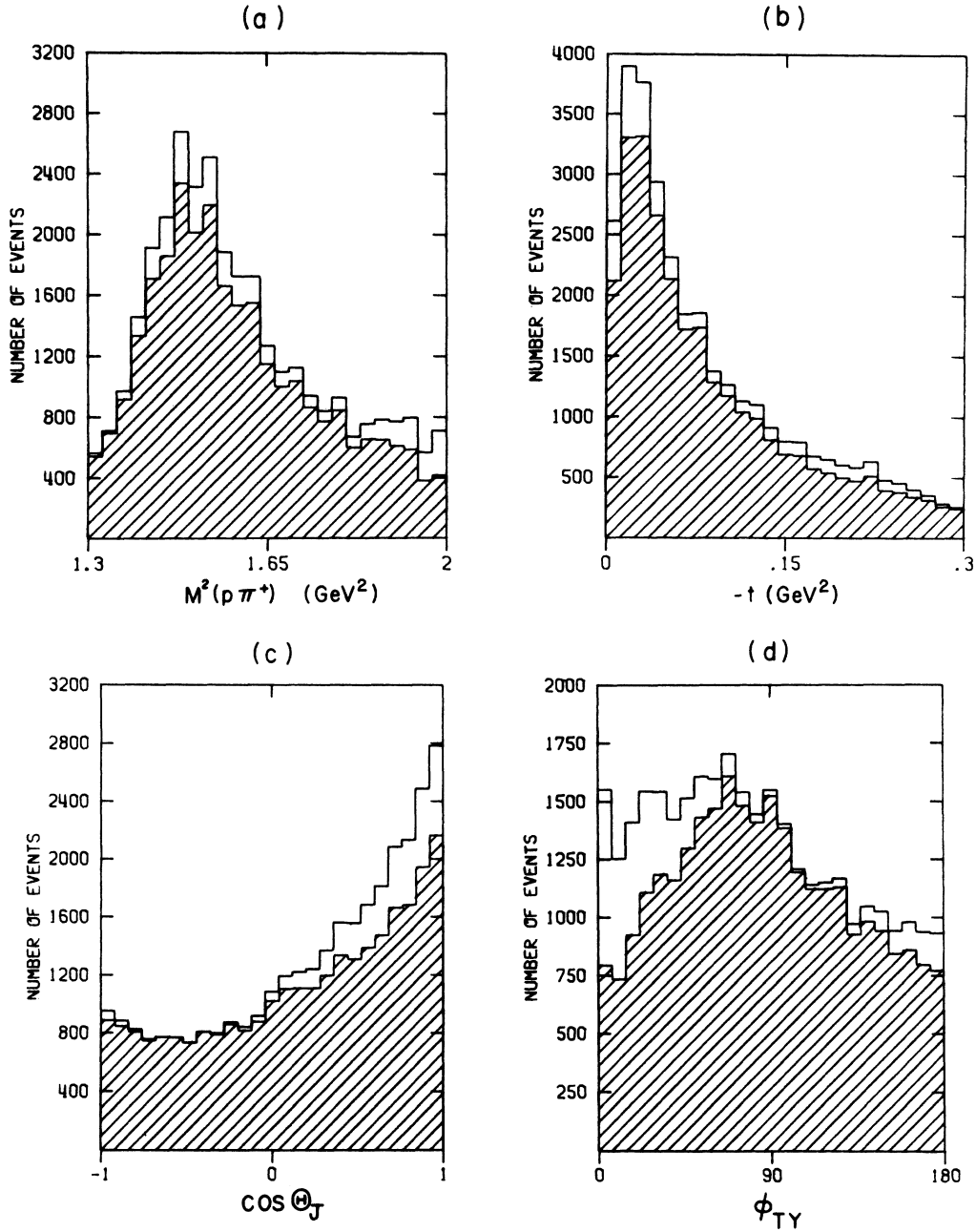


FIG. 3. Distributions in (a) $M^2(p\pi^+)$; (b) $-t$; (c) $\cos\theta_J$, and (d) ϕ_{TY} for reaction (1) before (shaded) and after (all) experimental corrections.

over-all χ^2 for the two sets of data is relatively poor.

Figures 3(c) and 3(d) show the θ_J and ϕ_{TY} distributions, respectively. The nonisotropic ϕ_{TY} distribution is evidence against the simple one-pion-exchange model and has been shown to be consistent with the double-Regge-pole model or the Reggeized pion-exchange model in the version of Berger.²⁵

The " $t\sigma$ " values defined in Eq. (17) were calculated using the off-mass-shell scattering data and the Chew-Low, Dürr-Pilkuhn, and Benecke-Dürr cross-section parameterizations. Fits constrained to pass through the origin were made assuming linear, quadratic, and cubic extrapolation polynomials. Figure 6 shows the Benecke-Dürr quadratic fit results. The results obtained using the Dürr-Pilkuhn model were similar.

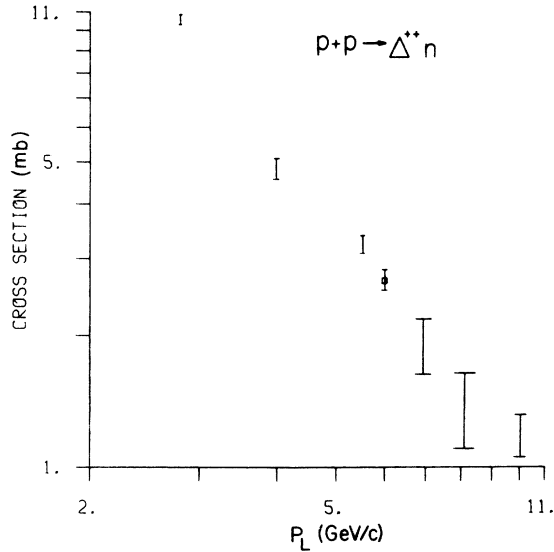


FIG. 4. Cross sections for reaction (1), including the measurement of this experiment at 6 GeV/c.

The Chew-Low fits were generally quite poor, as were all linear fits. Table III summarizes the results of a comparison between the eight extrapolated and known on-mass-shell cross sections. The χ^2 is smallest for the Dürr-Pilkuhn and Benecke-Dürr quadratic fits.

The three polynomial extrapolation terms used above all require explicitly that the " t " curve be zero at $t=0$. Several schemes have been proposed to account for the possible deviation of the OPE differential cross section from zero at $t=0$. It has been proposed²⁶ that conspiracy could occur between the pion Regge pole and an opposite parity pole which can lead to effects similar to damping corrections in absorption models. The mod-

TABLE I. Number of events after experimental correction for $M_{p\pi}$.

$M_{p\pi}$ (GeV)	Events
1.14-1.16	4980
1.16-1.18	9863
1.18-1.20	16 023
1.20-1.22	21 296
1.22-1.24	23 197
1.24-1.26	18 922
1.26-1.28	16 218
1.28-1.30	12 196
1.30-1.32	10 872
1.32-1.34	9 549
1.34-1.36	7 262
1.36-1.38	7 875
1.38-1.40	6 304
1.40-1.42	4 795

ifications necessary to have $d\sigma/dt$ not pass through zero at $t=0$ also arise naturally from the absorption model,²⁷⁻²⁹ although specific calculations suggest that the cross section may differ only slightly from zero at these energies.³⁰ Previously, pole extrapolations not required to pass

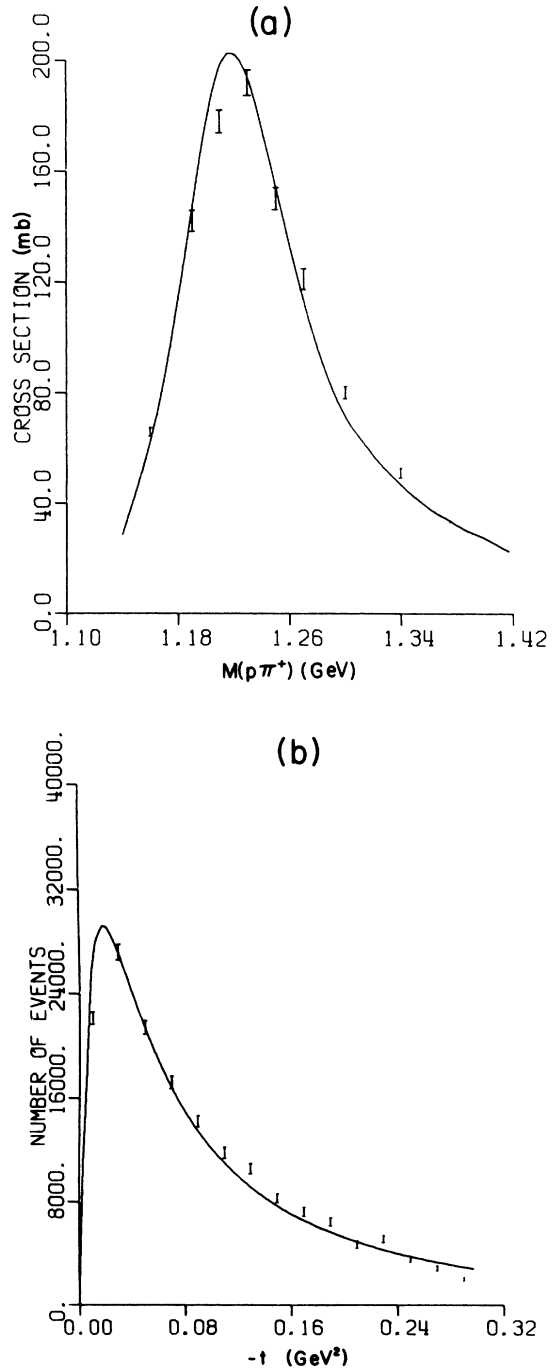


FIG. 5. Comparison between the (a) $M(p\pi^+)$ and (b) $-t$ distributions of reaction (1) and the Dürr-Pilkuhn model.

TABLE II. Number of events after experimental correction for t distribution.

$-t$ (GeV^2)	Events
0.0–0.02	22115
0.02–0.04	27204
0.04–0.06	21399
0.06–0.08	17197
0.08–0.10	14220
0.10–0.12	11763
0.12–0.14	10579
0.14–0.16	8277
0.16–0.18	7216
0.18–0.20	6417
0.20–0.22	4666
0.22–0.24	5088
0.24–0.26	3538
0.26–0.28	2828
0.28–0.30	1988

through the origin could not be accomplished with enough precision to detect a nonzero cross-section contribution at $t=0$.⁵ The data presented here provide a statistically significant test of that question. The extrapolated “ $t\sigma$ ” values at $t=0$, obtained with data normalized by the Dürr-Pilkuhn and Benecke-Dürr model calculations, and not required to pass through the origin, are consistent

TABLE III. χ^2 values (per eight degrees of freedom) for comparison between pole-extrapolated cross sections and on-mass-shell cross sections. The pole-extrapolated cross sections are based on Chew-Low (CL), Dürr-Pilkuhn (DP), and Benecke-Dürr (BD) models with At , $At+Bt^2$, and $At+Bt^2+Ct^3$ fits to “ $t\sigma$ ” (constrained to pass through the origin).

	At	$At+Bt^2$	$At+Bt^2+Ct^3$
CL	2519	130	59
DP	63	15	27
BD	109	13	25

with zero as an examination of the χ^2 values in Table IV will verify.

V. CONCLUSIONS

This paper reports on a high statistics analysis of the reaction $pp \rightarrow \Delta^+(1236)n$ at an incident proton momentum of 6 GeV/c. Emphasis has been given to an analysis of the data in terms of the basic Chew-Low one-pion-exchange mechanism and modifications thereof according to the form-factor models of Dürr-Pilkuhn and Benecke-Dürr. It is found that both form-factor models give good fits to the data. In addition, it is found that the

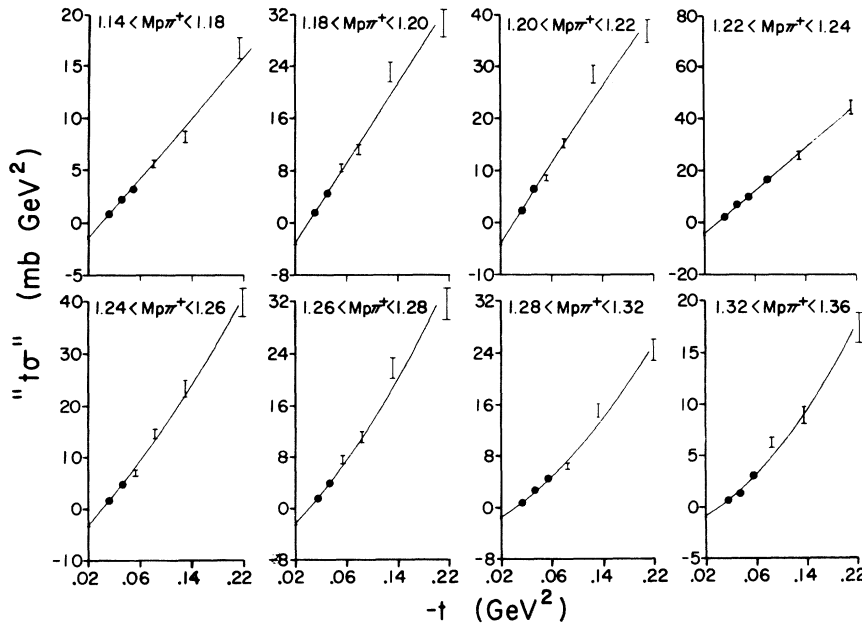


FIG. 6. Fits to “ $t\sigma$ ” versus $-t$ based on the Benecke-Dürr model for quadratic extrapolations to the pion pole. All fits were constrained to pass through “ $t\sigma$ ”=0 at $t=0$. The errors on the lower points are equal to the size of the points.

TABLE IV. χ^2 values (per eight degrees of freedom) for comparison between pole-extrapolated cross sections and on-mass-shell cross sections. The pole-extrapolated cross sections are based on Chew-Low (CL), Dürr-Pilkuhn (DP), and Benecke-Dürr (BD) models with $A + Bt$ and $A + Bt + Ct^2$ fits to " $t\sigma$ " (not constrained to pass through the origin).

	$A + Bt$	$A + Bt + Ct^2$
CL	1114	14
DP	59	11
BD	96	11

form-factor models in conjunction with quadratic extrapolations in t reproduce the known on-mass-shell dependence of the cross section for elastic π^+p scattering.

ACKNOWLEDGMENTS

The authors acknowledge the very important contributions of the Argonne National Laboratory ZGS staff during the data-taking phase of this experiment. The considerable support of the Michigan State University Computer Center was vital to the successful completion of the analysis of the data.

*Work supported in part by the National Science Foundation and the U. S. Energy Research and Development Administration.

†Presently at Department of Biophysics, Michigan State University, East Lansing, Michigan 48824.

‡Presently at NMCSSC-DCA, Pentagon, Washington, D.C.

§Presently at Lawrence Berkeley Laboratory, Berkeley, California 94720.

|| Presently at Department of Physics, Louisiana State University, Baton Rouge, Louisiana 70803.

¹H. P. Dürr and H. Pilkuhn, *Nuovo Cimento* **40A**, 899 (1965).

²J. Benecke and H. P. Dürr, *Nuovo Cimento* **56A**, 269 (1968).

³G. F. Chew and F. E. Low, *Phys. Rev.* **113**, 1640 (1959).

⁴Gunter Wolf, *Phys. Rev. Lett.* **19**, 925 (1967); *Phys. Rev.* **182**, 1538 (1969).

⁵Z. Ming Ma *et al.*, *Phys. Rev. Lett.* **23**, 342 (1969), and references cited therein.

⁶J. D. Jackson and H. Pilkuhn, *Nuovo Cimento* **33**, 906 (1964).

⁷For a detailed compilation of data, see E. Flaminio *et al.*, CERN Report No. CERN/HERA 70-5, 1970 (unpublished).

⁸A. A. Carter *et al.*, *Nucl. Phys.* **B26**, 445 (1971).

⁹R. J. Eden, *High Energy Collisions of Elementary Particles* (Cambridge Univ. Press, Cambridge, England, 1967), Chap. 3.

¹⁰J. D. Jackson, *Nuovo Cimento* **34**, 1644 (1964).

¹¹M. Jacob and G. Chew, *Strong Interaction Physics* (Benjamin, New York, 1964), Chap. 1.

¹²E. Colton, thesis, University of California, Los Angeles, 1968 (unpublished), Appendix A.

¹³J. Blatt and V. Weisskopf, *Theoretical Nuclear Physics* (Wiley, New York, 1952), p. 358.

¹⁴CRUNCH is a filter program written by J. Prukop, University of Notre Dame, Ph.D. thesis, 1973 (unpublished).

¹⁵D. E. C. Fries, *Nucl. Instrum. Methods*, **44**, 317 (1966).

¹⁶D. E. C. Fries, SLAC Report No. SLAC-99, UC-34 (EXPI), 1969 (unpublished).

¹⁷I. Derado and R. Leedy, SLAC Report No. SLAC-72, UC-34, Physics TID-4500 (49th edition) (unpublished).

¹⁸H. A. Bethe, *Phys. Rev.* **89**, 1256 (1953).

¹⁹E. Segrè, *Experimental Nuclear Physics* (Wiley, New York, 1953), p. 287.

²⁰L. Marten, *Methods of Experimental Physics* (Academic, New York, 1961), p. 73.

²¹L. Landau, *J. Phys.* **8**, 201 (1944).

²²B. Rossi, *High Energy Particles* (Prentice-Hall, Englewood Cliffs, New Jersey, 1952).

²³Y. K. Akimov, *Scintillation Counters in High Energy Physics* (Academic, New York, 1965).

²⁴O. Benary, L. Price, and G. Alexander, University of California Radiation Laboratory Report No. UCRL-20000 NN, 1970 (unpublished).

²⁵P. Kobe *et al.*, *Nucl. Phys.* **B52**, 109 (1974).

²⁶R. J. N. Phillips, *Nucl. Phys.* **B2**, 394 (1967).

²⁷G. L. Kane, *Phys. Rev. Lett.* **25**, 1519 (1970).

²⁸V. Blobel *et al.*, *Nucl. Phys.* **B67**, 284 (1973).

²⁹F. Wagner, *Nucl. Phys.* **B58**, 494 (1973).

³⁰S. Hagopian *et al.*, *Phys. Rev. D* **7**, 1271 (1973).